Borrower: YUS

Lending String: *ORN,ORN

Patron: Michael Wilson

Journal Title: Proceedings of sixth Joint Workshop on Electron Cyclotron Emission and Electron Cyclotron Resonance Heating, Oxford, 16-17 September 1987.

Volume: 6 **Issue:**
Month/Year: September 1987 **Pages:** 23-30

Article Author: Joint Workshop on Electron Cyclotron Emission and Electron Cyclotron Resonance Heating (6th ; 1987 ;

Article Title: N Fisch, A Kritz, M Gerstein; Inverse Problem for Synchrotron Radiation in the Presence of Noise

Imprint: [S.l. ; s.n., 1987?]

ILL Number: 36747280

Call #: QC718.5.C9 .I5x 1987

Location: Main

~~E-Mail~~ Ariel
Charge: 0
Maxcost: $50IFM

Shipping Address:
Yale University
Kline Science Library, ILL
219 Prospect Street (P.O. Box 208111)
New Haven, CT 06520-8111

Fax: 203-432-2257 (b
Ariel: 130.132.32.199
Email: grace.epps@yale.edu

✓

CLM-ECR (1987)

PROCEEDINGS OF SIXTH JOINT WORKSHOP ON

Electron Cyclotron Emission and Electron Cyclotron Resonance Heating

OXFORD, 16 – 17 SEPTEMBER 1987

Inverse Problem for Incremental Synchrotron Radiation in the Presence of Noise

EC-6
OXFORD

N.J. Fisch, A.H. Kritz and M. Gerstein
Plasma Physics Laboratory, Princeton University, Princeton, NJ 08544

Plasma synchrotron emission can be used to diagnose important momentum space features of high energy electrons. One way in which this radiation might be used relies on the measurement of the 2-D pattern $R(\omega,\theta)$ of radiation emitted at frequency ω into angle θ, where θ measures the angular deviation from purely perpendicular observation of the magnetic field. (The tokamak is observed in the vertical plane that includes the tangent to the magnetic field **B**, so the strength of **B** may be assumed constant and known.) The 2-D pattern $R(\omega,\theta)$ might then be used to infer the two-dimensional electron distribution function $f(p_{\|},p_{\perp})$, where $p_{\|}$ and $p_{\perp}$ refer to the electron momentum, respectively, parallel and perpendicular to the magnetic field. This approach, however, suffers because it requires the deployment of an array of microwave detectors to resolve the θ-dimension. In practice, possibly only one detector is available, and, while it has been used to place useful constraints[1-6] on $f(p_{\|},p_{\perp})$, or to deduce elegantly[7] a 1-D f, a full inversion is not possible.

A second way to obtain information might be to employ rf or other power to induce in the plasma a momentum-space flux $\mathbf{\Gamma}(\mathbf{p},t)$, and to measure the *incremental* radiation emitted by the perturbed distribution, i.e., the additional radiation produced as a result of the probing rf power. One can then pose the following problem: to deduce the momentum space details of the source function, $\mathbf{\Gamma}(\mathbf{p},t)$, given this incremental radiation. Details of this source function give the velocity space details of power absorption, which may be of immediate interest in rf heating or current drive experiments. Also, the details of the absorption informs on the electron distribution function itself, since, basically, where (in velocity space) power is absorbed, there must be electrons.

To isolate the incremental radiation, we are at liberty to modulate or otherwise to control the time-dependence of the source; so suppose we impose an impulse $\mathbf{\Gamma} = \mathbf{S}(\mathbf{p})\delta(t)$. The incremental radiation now decays in time as the electrons suffer collisions, obeying laws we think we know, so that this time decay reveals the details of the original impulse. For example, incremental radiation associated with fluxes of fast electrons decays slowly; for nonrelativistic electrons the decay time goes as $1/p^3$. If there are N time points collected during the electron slowing-down time, then the 2-D impulse response, $R(\omega,t)$, produces N times the constraints on $\mathbf{S}(\mathbf{p})$ than does the immediately available spectra $R(\omega,t=0)$. Thus, using only one observation angle, we hope to deduce the 2-D wave-induced flux $\mathbf{S}(\mathbf{p})$ from the 2-D radiation data, $R(\omega,t)$. Of course, if more detectors were available, the multiplication in information would be the same, and the additional information might be used to uncover spatial dependencies.

In Fig. 1 we show the incremental radiation associated with a narrow incremental distribution of electrons centered around 150 keV and with energy almost entirely in the parallel direction. Here, we view the extraordinary polarization of the radiation at an angle $\theta = 0$. Beneath the radiation surface $R(\omega,t)$, we project the frequency at which the maximum radiation occurs as a function of time. Traces such as this look different at different θ or given different incremental electron distributions. These differences are to be exploited in trying to deduce from the radiation the initial conditions. Alternatively, it may also be of interest to try to deduce the viewing angle.

The general problem is to deduce the perturbation **S** from the radiation data R when the radiation is observed at some arbitrary angle θ. However, an important simplification occurs when $\theta = 0$, i.e., when the viewing is purely perpendicular. In this case, all electrons at the same energy radiate at the same frequency, because the radiation is not Doppler shifted. Moreover, in the absence of a dc electric field, such as might occur in a steady state tokamak, superthermal electrons slow down as a function of energy only, while diffusing very little in energy. Thus, electrons initially at the same energy lose energy at the same rate, and so both initially and subsequently radiate at the same frequency, irrespective of scattering in pitch-angle. It is possible then to take a projection of the data $r(t) = R(\omega(t), t)$, such that the frequency $\omega(t)$ tracks in time the incremental radiation associated with a perturbation initially at one energy. The equation to be solved may be written as

$$r(\tau) \equiv R(\omega(\tau), \tau) = \frac{e^2\omega}{c} \sum_k \gamma^2(u) Q_k(u) \left(\frac{\gamma(u)+1}{u}\right)^{\alpha_k} \left(\frac{\rho}{\gamma(\rho)+1}\right)^{\alpha_k} \frac{\rho^3}{\gamma^2(\rho)} H_{nk}(\rho), \quad (1)$$

where, from the data $r(\tau)$, we seek to deduce the Legendre harmonics $Q_k(u)$ of the source function. In Eq.(1), the normalized momentum u enters as a parameter. The function H_{nk} is known, and the variable ρ is a function of u and normalized time τ. Here n is the predominant cyclotron harmonic at which emission occurs. In the event that several harmonics dominate, it would be necessary to sum the right hand side of Eq.(1) over n. It turns out, however, that one harmonic often dominates for *incremental* radiation, in which case Eq.(1) may be solved for the Q_k rather easily.

A detailed derivation and an analytic solution of Eq.(1) is given in Ref. 8. Here, we consider several questions relating to the viability of this technique. One issue is that of harmonic overlap: To what extent can the radiation by relativistic electrons at the observed frequencies be considered to be dominated by just a single cyclotron harmonic? In Fig. 2 we plot the frequency of radiation emitted by electrons as a function of time and parameterized by the initial energy of the electron. We consider initial electron energies in the range 250–500 keV. Initially, these electrons emit radiation at different frequencies; for example, the 500 keV electrons are relativistically the heaviest ($\gamma = 2$), so they emit at frequencies corresponding to the half-cyclotron frequencies rather than at the cyclotron frequencies. Also, initially being the most energetic, they slow down more slowly than do other electrons, so the frequency with which they emit changes more slowly in time than the frequency with which slower electrons emit. Eventually, of course, all electrons slow down to nonrelativistic frequencies, at which point they all radiate at the cyclotron harmonics. Thus, all the solid curves corresponding to each harmonic converge within an energy slowing down time of the 500 keV electrons.

The simplifying assumption concerning the dominance of one harmonic may now be checked for the following illustrative example: suppose *e.g.*, a 10 keV plasma in which tail electrons in the 250 – 500 keV range are (incrementally) rf heated, as might be contemplated in diagnosing a current-drive experiment. Let us further consider the case in which the diagnosis of the plasma is to be made on the basis of only the third harmonic radiation. At these energies this radiation initially fills the frequency regime of 1.5 to 2 Ω_e, as we can see from the figure.

Note first that the incremental radiation (3rd harmonic) associated with electrons at energies around 400 keV will be entirely untangled from the incremental radiation at any other harmonic associated with any of the excited electrons. This is because 2nd harmonic radiation even from the less energetic electrons (at 250 keV) is at too low a frequency to be confusable, while fourth harmonic radiation even from the more energetic electrons (at 500 keV) is at too high a frequency to be confusable. And while those 250 keV electrons do slow down, and then (2nd harmonic) radiate at a frequency that would have been confusable with radiation (3rd harmonic) from 400 keV electrons, note that by the time that happens, the electrons initially at 400 keV have now slowed down too, and are thus radiating at a higher frequency too. So there is no overlap. Moreover, this slowing down of the 400 keV electrons is still not fast enough to catch up with the fourth harmonic radiation of the 500 keV electrons, which are also slowing down and radiating at an even higher frequency. Thus, the conditions for the analytic inversion based on third harmonic emission are immediately satisfied for a source function in the vicinity of 400 keV. This vicinity, as can be seen, extends from about 350 keV to 500 keV. (At 500 keV there is some degradation of the data when the 500 keV electrons have slowed down to the point where they radiate at $2\Omega_e$, where there is some confusability with radiation from 2nd harmonic radiation from electrons originally at 250 keV, but the fraction of time points which are affected here appears to be small, about 10%.)

So, in this example, there is no confusion in finding on the basis of third harmonic radiation the details of the source function, $Q(p_{\|}, p_{\perp})$, in the energy range 350–500 keV. What about at the lower range 250–350 keV? At first glance this appears more difficult, at least based on just 3rd harmonic radiation, since 4th harmonic incremental radiation, particularly from electrons initially at 400–450 keV, is confusable over a significant portion of the slowing down trajectory. However, since the source function for radiation from 400–450 keV electrons has already been deduced, the contribution at the 4th harmonic by these electrons may be calculated and subtracted from the total observed radiation. The remainder is attributable to 3rd harmonic emission, so the conditions are met also for performing the analytic inversion in the 250–350 keV range.

In the above example, using the 2nd harmonic emission might have been more direct, but the 3rd harmonic radiation is often more reliable data. In any event, this example illustrates how the range of applicability of this inverse procedure may be extended beyond what appears available at first glance. In actuality, data from the higher harmonics can be quite useful;. In the limit that the additional data is not overlapping in frequency, it is roughly equivalent to having twice the number of independent data points. If there is significant overlap, a more complicated inverse problem must be solved, and there will be a tradeoff between the amount of additional data and the added confusability.

A second question of importance is the sensitivity of the data inversion to noise. The data inversion here is technically *ill-posed*,[9] so that care must be taken in performing the inversion. First, let us make a connection to more standard equations of the ill-posed type.

The 1-D projection equation can be understood as follows: Assume a distribution of electrons $f(\mu, t)$ that corresponds to a shell of electrons initially at some momentum u_0. The angular distribution relaxes according to an equation of the form

$$\frac{\partial f(\mu,t)}{\partial t} = D(u)\frac{\partial}{\partial \mu}(1-\mu^2)\frac{\partial}{\partial \mu}f(\mu,t), \tag{2}$$

where the diffusion coefficient D goes *e.g.*, as $1/u^3$ in the nonrelativistic limit. Now, as this shell distribution relaxes in μ, it also slows down in energy, so that it radiates at different frequencies. The radiation as a function of time may be put into the form

$$r(t) = \int f(\mu,t)I(\mu,\omega,u)d\mu, \tag{3}$$

where the known weighting function I is the radiated power of a single electron, and its arguments, $u = u(t)$ and $\omega = \omega(t)$ track the speed of the electron shell and the frequency with which they emit radiation. It is an easy matter to solve Eq.(2) given the initial condition $f(\mu, t = 0) = f_0(\mu)$, by summing over Legendre harmonics

$$f(\mu,t) = \sum_n a_n P_n(\mu) \exp\left[\frac{-n(n+1)\chi(t)}{2}\right], \tag{4}$$

where $\chi(t) = \int_0^t d\tau D(\tau)$, and where the a_n are the harmonics of the initial condition. Substituting now for $f(\mu,t)$ in Eq.(3), we can put $r(t)$ into the form

$$r(t) = \sum_n a_n \tilde{I}_n(t) \exp\left[\frac{-n(n+1)\chi(t)}{2}\right], \tag{5}$$

where $\tilde{I}_n(t)$ is the nth Legendre harmonic of the radiation function I.

The inverse problem that we pose is to deduce the a_n from the data $r(t)$. This is an ill-posed inversion, in that the higher harmonics will certainly be sensitive to small amounts of noise. A comparison of Eq.(5) with Eq.(4) is revealing. Eq.(4) represents the solution to a heat equation. For the forward posed equation, the data would be the a_n, from which we could deduce the solution $f(\mu,t)$. One standard backward posed equation would be to give $f(\mu, t = t_f)$ for some final time t_f, and then try to deduce the a_n, something that would succeed essentially for only the low n terms. What corresponds to our problem is a somewhat differently posed problem. Suppose that the data were given instead for $f(\mu = \mu_0, t)$ for some particular μ_0. The analogy to Eq.(5) would be exact were $\tilde{I}_n(t)$ independent of time, but the main features are present for $\tilde{I}_n(t)$ being merely a milder function of time than is the exponential function, $\exp[-(n(n+1)\chi(t))/2]$. In any event, the difficulty still remains in deducing the higher harmonics.

To get a feel for the number of harmonics that can be reliably inverted consider that the data $r(t)$ given at some finite number of time points, say M, is polluted by noise $\epsilon\tilde{r}(t)$, then how many harmonics a_n can be reliably inverted? Even without doing anything particularly sophisticated, we can see how the answer must scale: Any inversion scheme essentially uses data at long times to get the a_n for n small, and the data at short times to get the data for n large. Consider, for example, the effect of noise on the following recursive scheme for getting the a_n: suppose $a_0, a_1, \ldots a_{j-1}$ have been found — then look at the data at times such that $\exp[-j(j+1)\chi(t)/2] \sim O(1)$, but that $\exp[-n(n+1)\chi(t)/2] \ll 1, n > j$. We assume that the time dependence of $\tilde{I}_n(t)$ is mild. Then the harmonics higher than j contribute negligibly (corrections, if desired, could be found perturbatively) at such time values, while, by presumption, the harmonics lower than j have already been found — so the jth harmonic is deducible. The recursion proceeds by considering time data in the next interval, where $\exp[-(j+1)(j+2)\chi(t)/2] \sim O(1)$.

The procedure proceeds similarly in the presence of noise. Depending on the level and correlation of the noise, and the accuracy desired in the a_n, a number of time points are now required in each interval. Suppose that l time points are needed in each interval, and suppose that the time data is obtained every Δt. Define $\chi'(t) \equiv \partial\chi/\partial t$. Then we must have $\exp[-n(n+1)\Delta t\, l\chi'(0)/2] \sim O(1)$ to have l points with which to deduce the nth harmonic. This can be satisfied approximately for harmonics such that $n^2 < (l\Delta t\chi'(0))^{-1}$. Note that for the problem at hand, $\chi'(0) \sim (1+u_0^2)/u_0^2$, which is just the initial slowing down rate. Now if M time points are collected in the decay time of the slowest harmonic, we have $\Delta t\chi'(0) = 1/M$, so that harmonics satisfying the inequality $n^2 < M/l$ can be inverted. Suppose that the data $r(t)$ is described by, say, $M = 10^4$ time points. If we needed 10 points to deduce each harmonic, i.e. $l = 10$, then, by the inequality above, we expect to invert reliably about the first thirty Legendre harmonics. Actually, even several would be a significant advance over what is obtainable without the time information; five to ten would pin down many important details of the electron distribution in typical rf heating and current drive experiments.

We performed numerical inversions of Eq.(1) in the presence of numerically simulated noise. In Fig. 3 we show by means of the dashed line the incremental source function $Q(\mu)$, which represents the pitch angle dependence of an initial perturbation of electrons initially at about 150 keV. In the absence of noise, the data can be inverted essentially exactly – i.e., so as to infer a source function that, in fact, overlays the dashed line. In the presence of noise, we invert the data to obtain an estimate of $Q(\mu)$, which is the boxed line, which we note very nearly overlays the true source function.

The radiation data $r(t)$ that corresponds to the true source function is given in Fig. 4. In order to simulate noisy data, we added to each true data point a random number with zero mean and variance of about 20% of the maximum data value. Thus the uncertainty in each data point is very large except near the maximum radiation. The noisy data is shown in Fig. 5. This data was inverted to give the estimate of $Q(\mu)$ shown in Fig. 3. The number of harmonics used to represent $Q(\mu)$ is 10 and the number of time points here is 900. Here, the inversion evidently succeeds quite well in the presence of a relatively high level of uncorrelated noise.

This work was supported by United States Department of Energy under contract number DE–AC02–76–CHO3073. One of us (AHK) was supported in part by a DOE-ORAU Professional Development Grant.

---

[1] C. M. Celata and D. Boyd, Nucl. Fusion **17**, 735 (1977).

[2] S. Tamor, Nucl. Fusion **19**, 455 (1979).
[3] M. Bornatici, R. Cano, O. de Barbieri, and F. Englemann, Nucl. Fusion **23**, 153 (1983).
[4] C. M. Celata, Nucl. Fusion **25**, 35 (1985).
[5] I. H. Huchinson and K. Kato, Nucl. Fusion **26**, 179 (1986).
[6] K. Kato and I. H. Huchinson, Phys. Rev. Lett. **56**, 340 (1986).
[7] S. M. Mahajan, C. Oberman and R. C. Davidson, Plasma Phys. **16**, 1147 (1974).
[8] N. J. Fisch, Princeton Plasma Physics Laboratory Report PPPL-2457 (1987).
[9] A. N. Tikhonov and V. Y. Arsenin, *Solutions of Ill-posed Problems*, V. H. Winston, Washington, D.C., 1977.

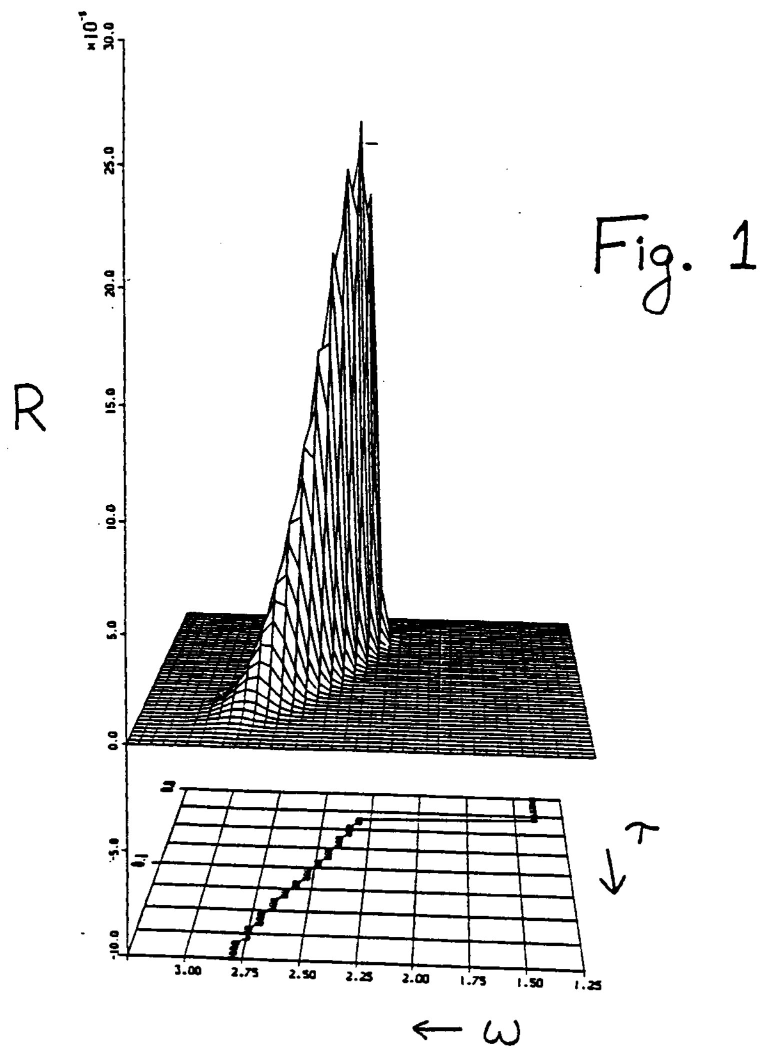

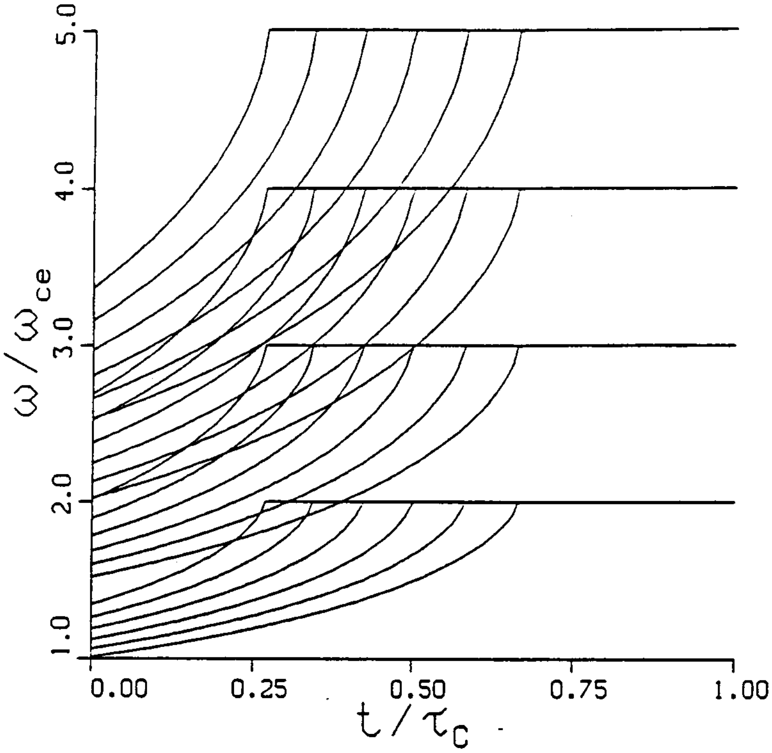

5.0
4.0
3.0
2.0
1.0
ω / ω_ce
0.00
0.25
0.50
0.75
1.00
t / τ_c

Fig. 2

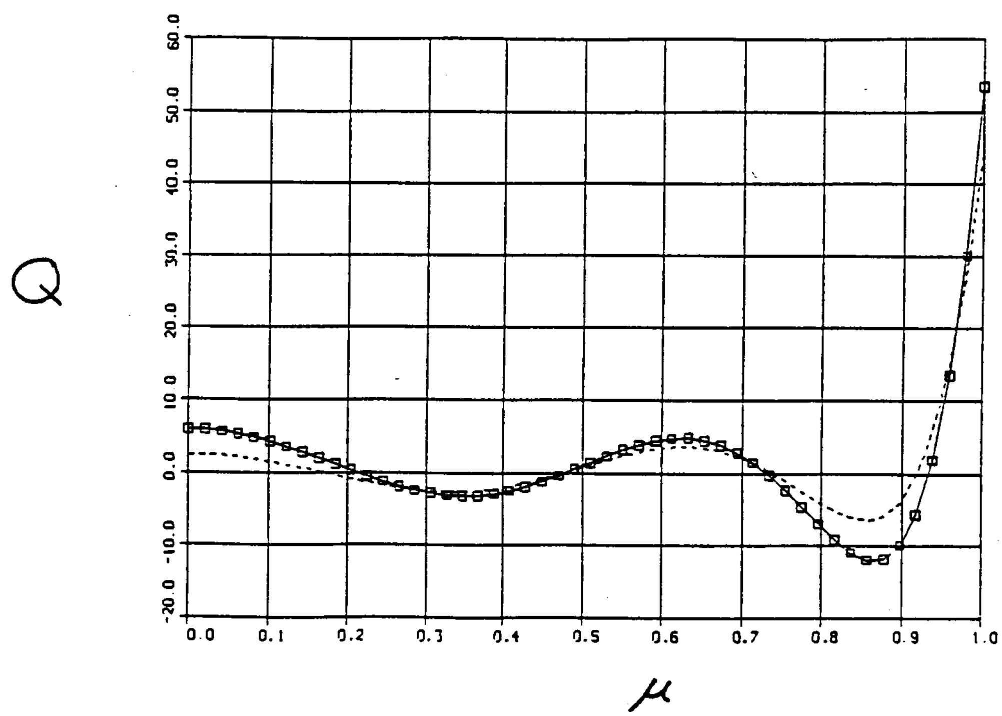

60.0
50.0
40.0
30.0
20.0
10.0
0.0
-10.0
-20.0
Q
0.0
0.1
0.2
0.3
0.4
0.5
0.6
0.7
0.8
0.9
1.0
μ

Fig. 3

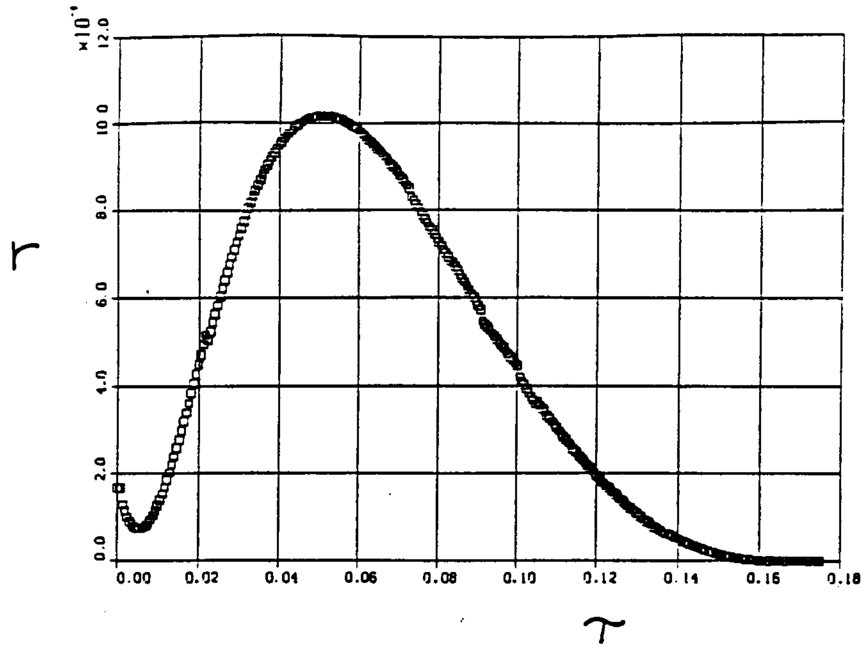

×10⁻¹
12.0
10.0
8.0
6.0
4.0
2.0
0.0
r
0.00
0.02
0.04
0.06
0.08
0.10
0.12
0.14
0.16
0.18
τ

Fig. 4

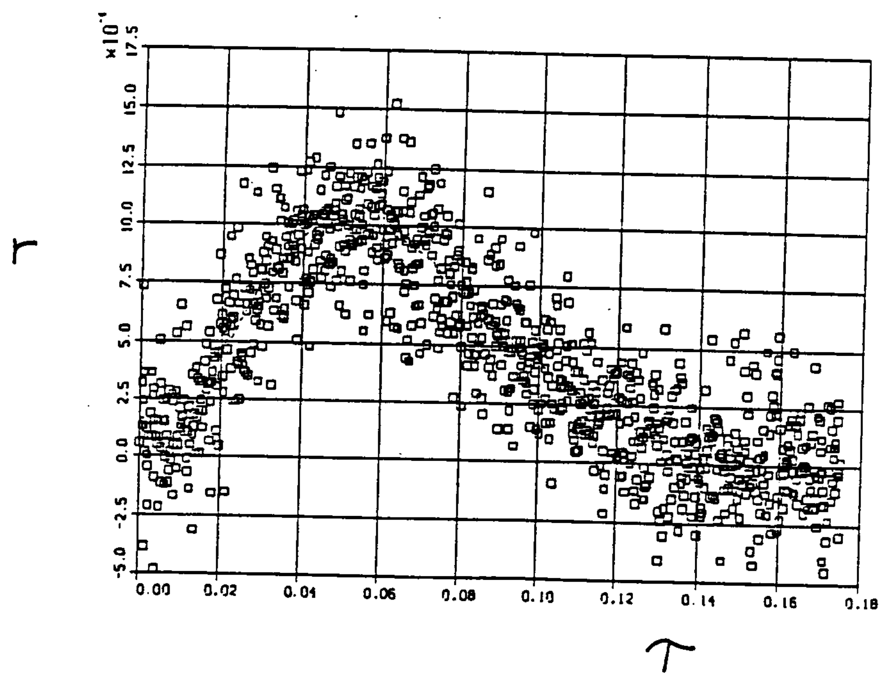

×10⁻¹
17.5
15.0
12.5
10.0
7.5
5.0
2.5
0.0
-2.5
-5.0
r
0.00
0.02
0.04
0.06
0.08
0.10
0.12
0.14
0.16
0.18
τ

Fig. 5